SAND2015-1540C

Highly Damped, Sinusoidal Long Fiber Composite Material Evaluation

Troy J. Skousen
Sandia National Laboratories
Program and Test Integration Department

Randall L. Mayes
Sandia National Laboratories
Structural Dynamics & X-ray/NDE Department

Peter G. Stromberg
Sandia National Laboratories
Advanced Flight Systems Department

William A. Fladung
ATA Engineering, Inc.

Marcus D. Billings
ATA Engineering, Inc.

ABSTRACT

An evaluation of damped composite was performed. The composite material utilizes constrained layer damping with viscoelastic layers. The composite has the long fibers placed in sinusoids or waves. When the viscoelastic layer is sandwiched between composite layers with opposing sinusoids, deflections of the sinusoids due to vibration loading result in local shearing of the viscoelastic material. This shearing generates high structural damping. The damped material evaluation consisted of modal tap testing to down select from several composite tubes with varying sinusoid spatial period and amplitude. In depth modal testing was then performed on two damped tubes and one undamped tube. The peak damping for the axial and bending modes of the wavy composite tubes was 30 to 48 times higher than the undamped tube. Increased damping values were incorporated in to modal random vibration analysis and acoustic analysis to gauge the effectiveness of the increased damping in the final design loads. The largest reduction in design loads due to increased damping was 14%.

ACKNOLEDGEMENTS

The authors want to thank Dr. William (Bill) F. Pratt at Western Illinois University for lending the damped wavy composite tubes so that this testing could be performed.

OVERVIEW

Composite structures are commonly used in structural design, as they are strong and light weight. These structures can be exposed to significant environment loading. With the significant loading, high responses can be seen within the structure that can cause failure. It is prudent to look for ways to reduce the structural response. One way to reduce structural response is to add damping to the structure.

This report documents the methodology and results of the modal tests performed on a number of wavy composite tubes between May 28th, 2013, and May 31st, 2013, and between June 10th, 2013, and June 12th, 2013. The

* Sandia is a multiprogram laboratory operated by Sandia Corporation, a Lockheed Martin Company, for the United States Department of Energy under Contract DE-AC04-94AL85000

purpose of this testing was to obtain experimental data to evaluate the potential damping that could be obtained in a typical system component such as a strut.

The following sections will introduce the composite material tested, discuss the test procedure, and the conclusions from the testing.

MATERIAL INTRODUCTION

Constrained layer damping is a method to damp structures using viscoelastic materials. Viscoelastic materials resist shear strain motion by dissipating heat energy. When viscoelastic materials are included in structures such that they are exercised in shear, the damping in the structure will increase.

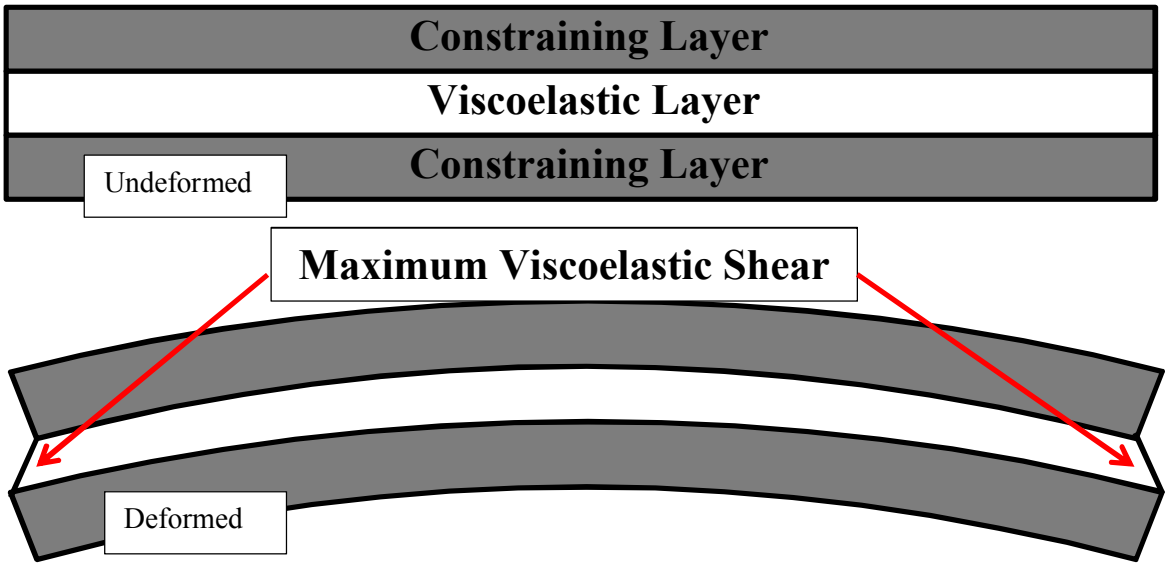

Figure 1: Side View of Traditional Constrained Layer Damping

In traditional constrained layer damping, as seen in Figure 1, a viscoelastic layer is sandwiched between two constraining layers of isotropic material. When the combined structure vibrates, it oscillates in bending, causing shear strain motion in the viscoelastic material. The shear strain increases with the relative deflection of the stiff materials on either side of the viscoelastic material. When there is no relative deflection, the viscoelastic does not have any shear strain motion and therefore the damping mechanism in the viscoelastic does not engage. In the case of a beam, as seen in the figure, the first bending mode of a structure usually has the largest deflection and therefore can cause the viscoelastic layer to provide the most damping. For the first bending mode, the constraining layers shear the viscoelastic the most near the tips of the beam while the middle of the beam does not shear the viscoelastic. In the case of uniform axial loading of a the constrained layer beam, the viscoelastic loading is only compressive or tensile and there would be little to no shear strain of the viscoelastic anywhere along the beam structure to incur damping.

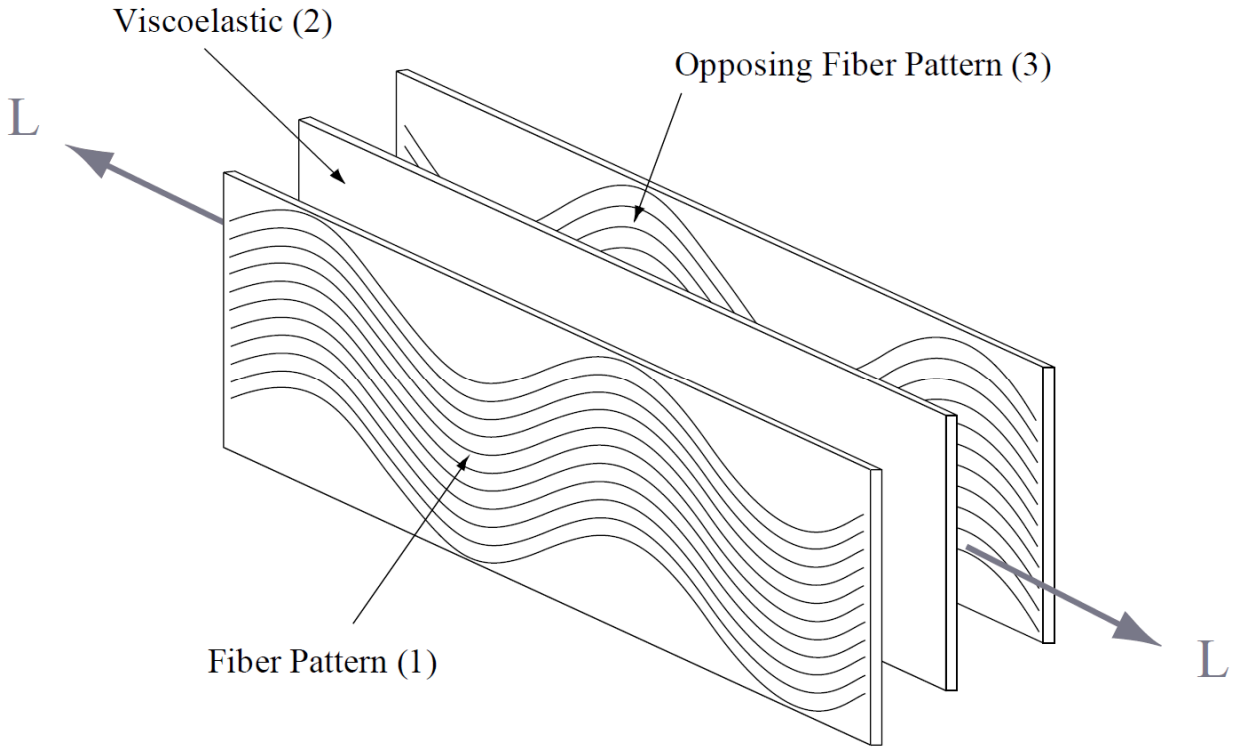

Figure 2: Dolgin Damped Wavy Composite Concept

Dolgin [1] suggested a way to shear the viscoelastic more uniformly throughout the structure under vibration loading. In his concept, shown visually in Figure 2, the viscoelastic layer (2) is still sandwiched between constraining layers (1, 3). The unique thing about the constraining layers is that they consist of long fiber composite materials where the long fibers are laid out in sinusoidal patterns. The key is that the sinusoid fiber pattern in the first constraining layer (1) is opposed, or 180° out of phase, to the sinusoidal fiber pattern in the other layer (3). As the structure deflects under loading, the sinusoids locally deflect in the opposite direction of the opposing layer, causing high shear strain motion in the viscoelastic layer throughout the structure. With this, even axial loading of the structure will cause this opposing local deformation of the sinusoids generating shear strain in the viscoelastic. The shear strain motion throughout the viscoelastic engages the damping mechanism more efficiently, which causes the inherent damping of the structure to increase.

TEST SAMPLES

Pratt [2] developed a machine that generates prepreg sheets of composite with sinusoidal patterns in the long fiber. Under a previous research contract, he made several samples of graphite tubes using the wavy prepreg sandwiching viscoelastic material following Dolgin's concept. Pratt provided several of the tubes to Sandia National Laboratories for testing by the modal group led by Randal Mayes.

Figure 3: Example Composite Tube Test Article

Figure 3 shows an example of one of the tubes that were provided for testing. The tubes were approximately 24 inches long with an inner diameter of 1 inch. Different tubes were made up of various layups of between 6 and 15 layers consisting of wavy graphite prepreg and viscoelastic layers. The graphite layers had sinusoids with various wave periods and maximum wave angles. Twelve tubes were available for testing. Table 1 shows the various layups indicating the wave length of the sinusoids, the maximum wave angle in the sinusoid, and the type of viscoelastic material used. The carbon fiber used for all of the layups was Grafil TR50S. The resin the fibers were imbedded into an Aldila sports resin, AR 250. The viscoelastic materials were of two types both from Avery Dennison, being UHA 1191 and UHA 1125. There is a key to understanding the nomenclature in the "Composite Layup" column of the table. The 'V' represents the viscoelastic layer. If there is a "2" in front of the V with '/' on either side of it, then there were two layers of viscoelastic put together. The standalone number on either side of the viscoelastic layers represent the number of in phase prepreg layers that were put together on one side of the viscoelastic. Prepreg layers that are on opposite sides of the viscoelastic layers are opposing sinusoid layers. The undamped tube (#3) was made of the same wavy prepreg material with no viscoelastic material. The sinusoidal properties in the undamped tube were not listed, because they do not affect the damping properties of the tube. Figure 4 points out the wave length and the wave angle of a sinusoid as described in the table.

Table 1: Wavy Composite Tube Test Sample Descriptions

Tube Number	Tube Name	Wave-Length	Wave Angle	Composite Layup	Viscoelastic Material
1	H4	1.5"	30°	3/2V/3	FT1125 (22 mil visco)
2	TR 21	5"	30°	3V3	FT1191
3	UN (Undamped Wavy)	1.5"	30°	Offset	N/A
4	TR 11	2"	30°	3V3	FT1191
5	TR 2	6"	30°	3V3	FT1191
6	TS	information unavailable			
7	H5	3"	30°	3V3	FT1125
8	TR 24	4"	30°	3V3	FT1191
9	TR 4	6"	30°	3V3V3V3	FT1191
10	TR 13	1.5"	30°	3/2V/3	FT1191 (22 mil)
11	TR 23	2"	22°	3V3	FT1191
12	TR 27	1.5"	30°	3/2V/3	FT1191 (22 mil visco)

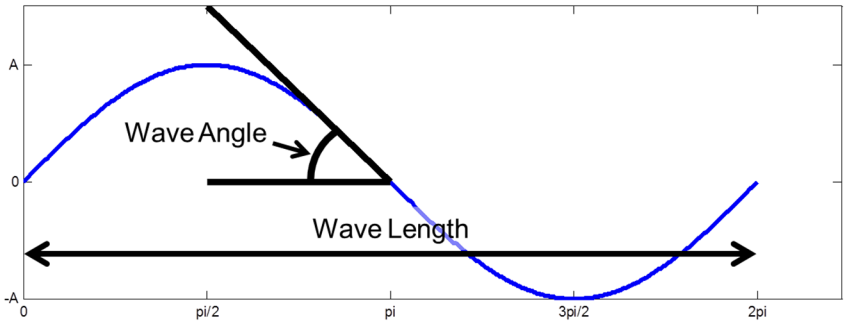

Figure 4: A Sinusoid Demonstrating the Wave Angle and the Wave Length

DOWN SELECT TESTING

There were not sufficient resources to perform in depth test evaluation of each of the tubes, so it was decided to down select from the 12 tubes to the one undamped tube and to two of the damped tubes. The rational for the down select of the two damped tubes was based on tap testing of the tubes with minimal instrumentation and with no additional test hardware that detailed testing would include. Figure 5 shows the test set up for this testing. Figure 6 shows the FRF test results from this round of testing. The critical damping ratio (expressed in percent) of the first mode of the undamped tube (tube 3) was 0.39%. Tubes 4 and 10 were selected for further testing with damping for the first mode of 6.83% and 7.07% respectively.

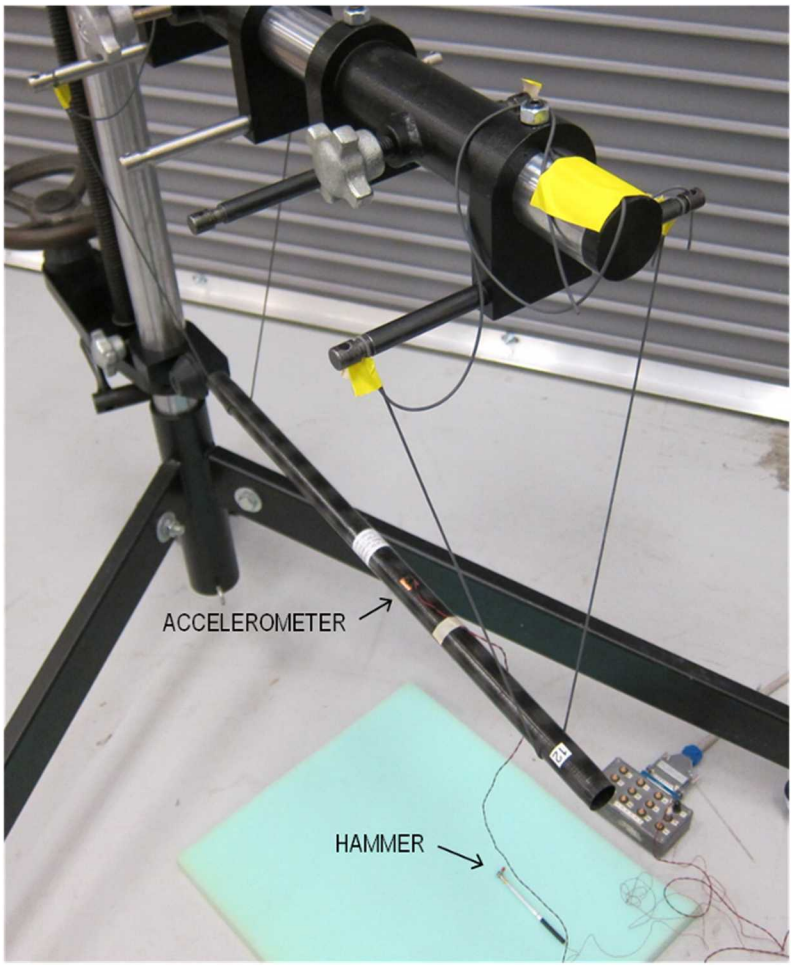

Figure 5: Down Select Test Setup

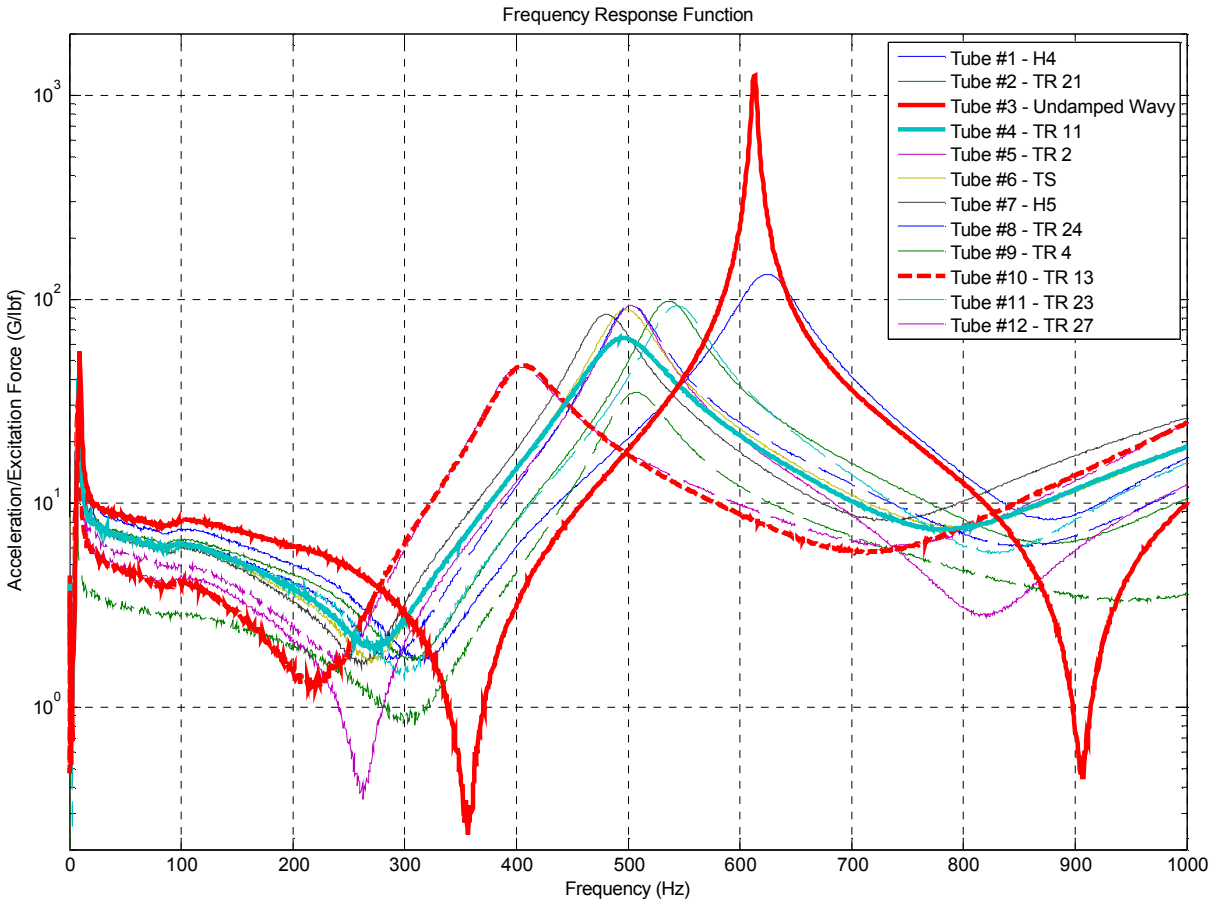

Figure 6: FRF Down Select Test Results

DETAILED TESTING

In the study that was conducted by Pratt, it was demonstrated that the damping of the wavy composite layups is frequency dependent in a manner similar to the example damping profile seen in Figure 7. There is a maximum damping at a particular frequency and the damping decreases as the frequency values move away from this frequency. In the detailed testing, the desire was to measure this damping profile by shifting the modes of the tubes and measuring the change in damping as the modes shifted.

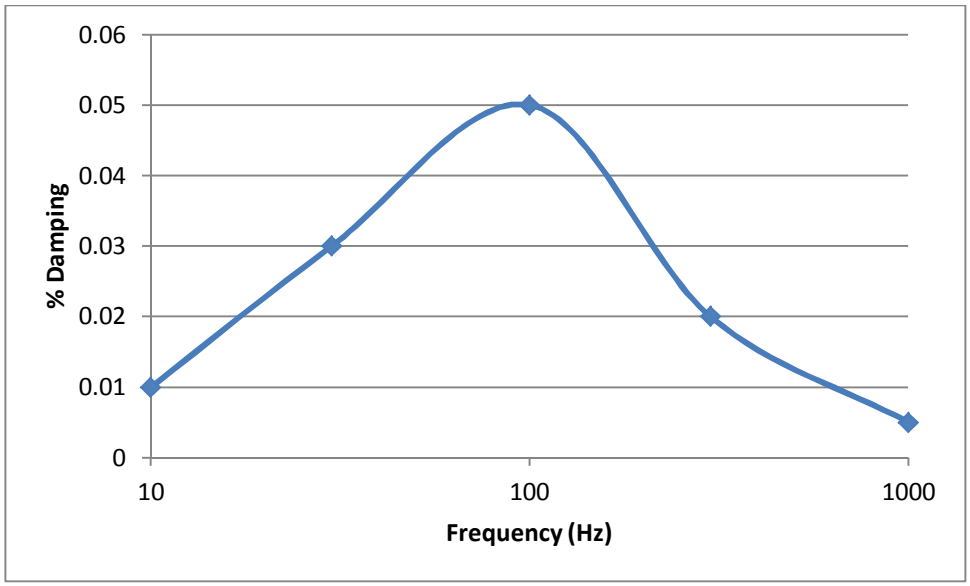

Figure 7: Typical Damping Profile

It was decided to shift the modes of the tubes by attaching weights of several masses to the end of the tubes. The masses used are seen in Figure 8. The set of masses consisted of an inner mass hub, which weighed 2 lbs., and was attached to the end of the tubes with an expanding collet. For the second set of masses, a small mass disk weighing 2 lbs. was attached to the inner hub to put 4 lbs. on each side of the tube. For the final set of masses, the small disk was replaced with a 14 lbs. disk to put 16 lbs. on each side of the tube. Input loads were applied to the tube/mass test articles with a force-measuring hammer. Cubes were attached to each of the masses so that torsion input loads could be applied with the hammer. Figure 9 shows the test set up for the detailed test series with 16 lbs. on each side of the tube. Accelerometers were attached to the masses to collect bending, axial, and torsional modes of the system.

Figure 8: Masses for Detailed Testing

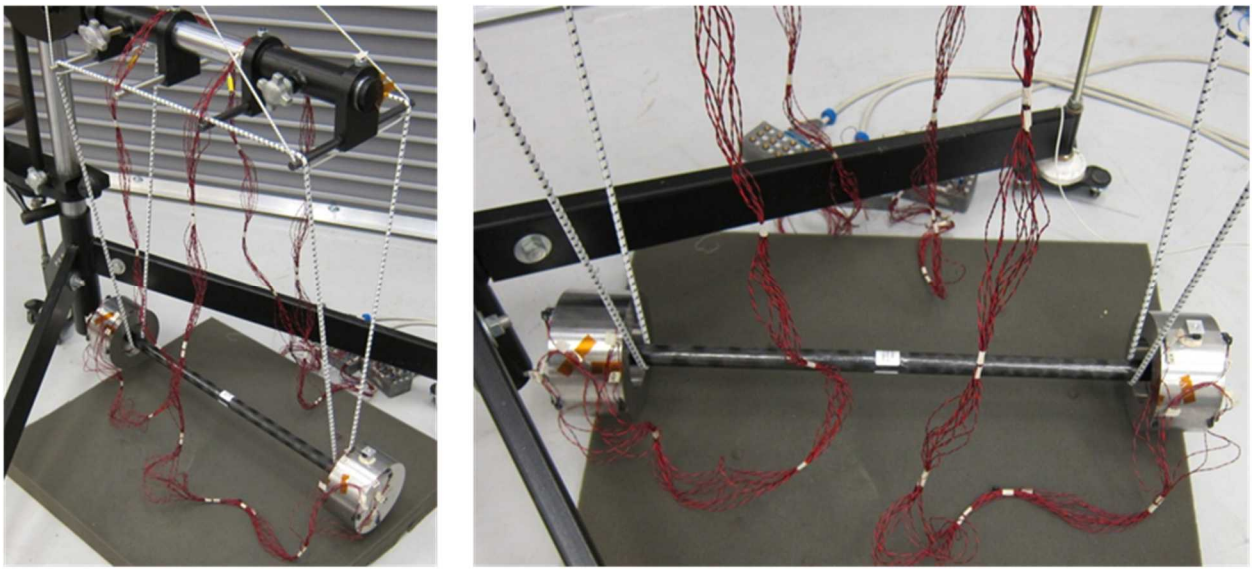

Figure 9: Detailed Test Setup

DETAILED TESTING RESULTS

Figure 10 shows response time history comparisons from a hammer tap on the undamped tube compared to a hammer tap on one of the undamped tubes with the 4 lbs. end masses. Note that the initial response is approximately the same for both responses indicating that the loading from the hammer was about the same for both tubes. Note also that the damped tube attenuates the response much more quickly than the undamped tube.

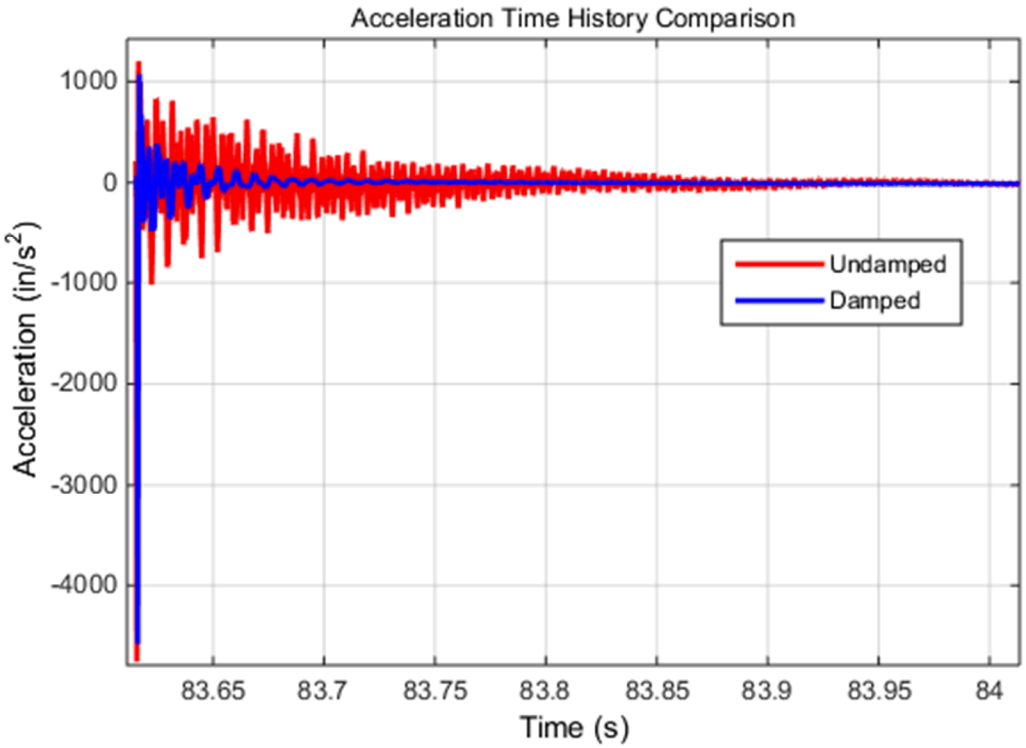

Figure 10: Times History Comparison Between Undamped and damped Tubes

The power spectrum mode indicator functions (PSMIF), which is the sum of the squared magnitude of all of the FRF, from the three configurations for the undamped Tube #3 are plotted in Figure 11. The identified modes are labeled. The 3rd bending modes with the 16 lbs. mass on the tubes were outside of the frequency range of the test and therefore are not included in the data. Also, note that since the test article is symmetric, the bending modes occur in pairs in the Y- and Z-directions at close frequencies. This can be seen in the double peaks for the 2nd and 3rd bending modes for the undamped tube with the 2 lb. end masses (circled in red). It would also be seen if one were to zoom in on the peak of the 1st bending mode. The PSMIFs show that the modes shift downward in frequency as the end mass increases and resonant frequencies of the three configurations cover a wide frequency range. The PSMIF from the three mass configurations for tube #4 and tube #10 are plotted in Figure 12 and Figure 13 respectively. The same information is plotted for each of the tubes by mode type in Figure 14, Figure 15, and Figure 16 and put in tables by mode type in Table 2 through Table 9.

The damping of the damped tubes was dramatically higher than the undamped tube. The largest difference in damping was for the axial mode of tube 10, which was a factor of 70 greater than the undamped tube.

Recall that one of the goals for these tests was to shift the frequencies of the modes with the different end masses to map out the damping profile that was expected to be similar to Figure 7. Figure 15 and Figure 16 show that with the three sets of end masses only part of the shape of the complete damping profiles could be mapped. For tube 4 in Figure 15 it looks like the peak of the damping profile was found for the 1st bending modes. The peak damping of the 2nd bending modes were not quite captured in the testing. For the 1st torsion and axial modes as well as the 3rd bending modes, the test results were clearly in the tail of the damping profiles. For tube 10 (Figure 16), the peak damping of the 1st axial mode and maybe the 1st bending modes were found. For the other modes, only damping values in one tail were found.

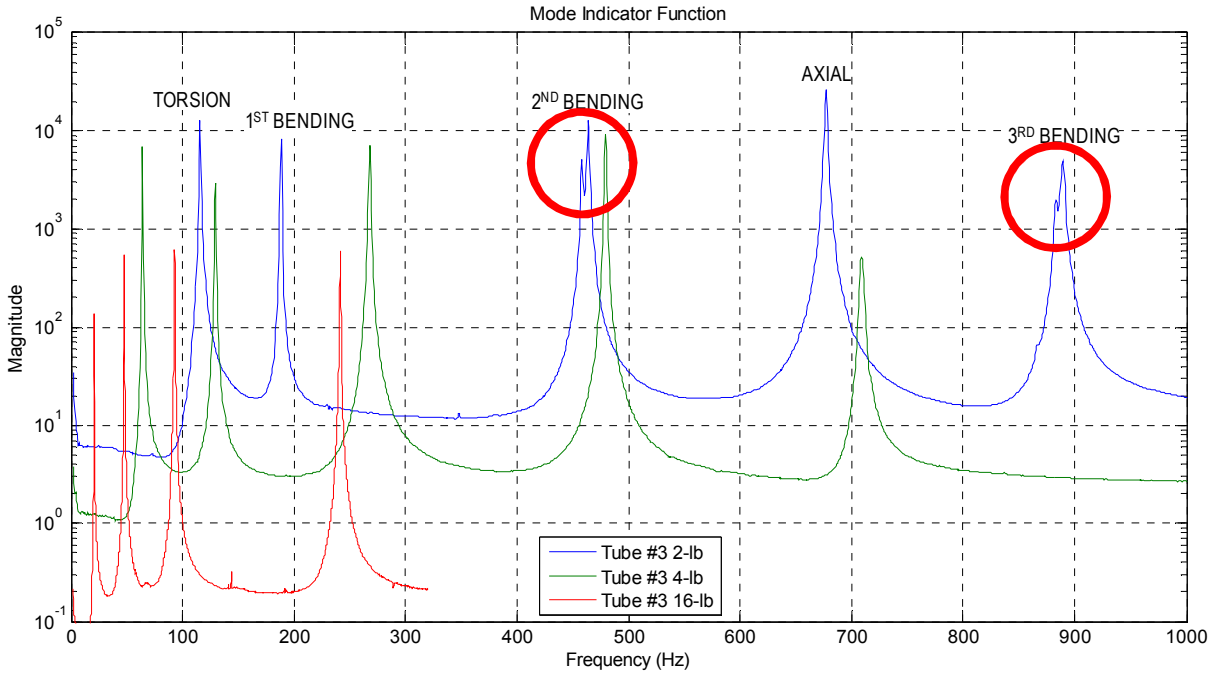

Figure 11. PSMIF from the three configurations for undamped Tube #3.

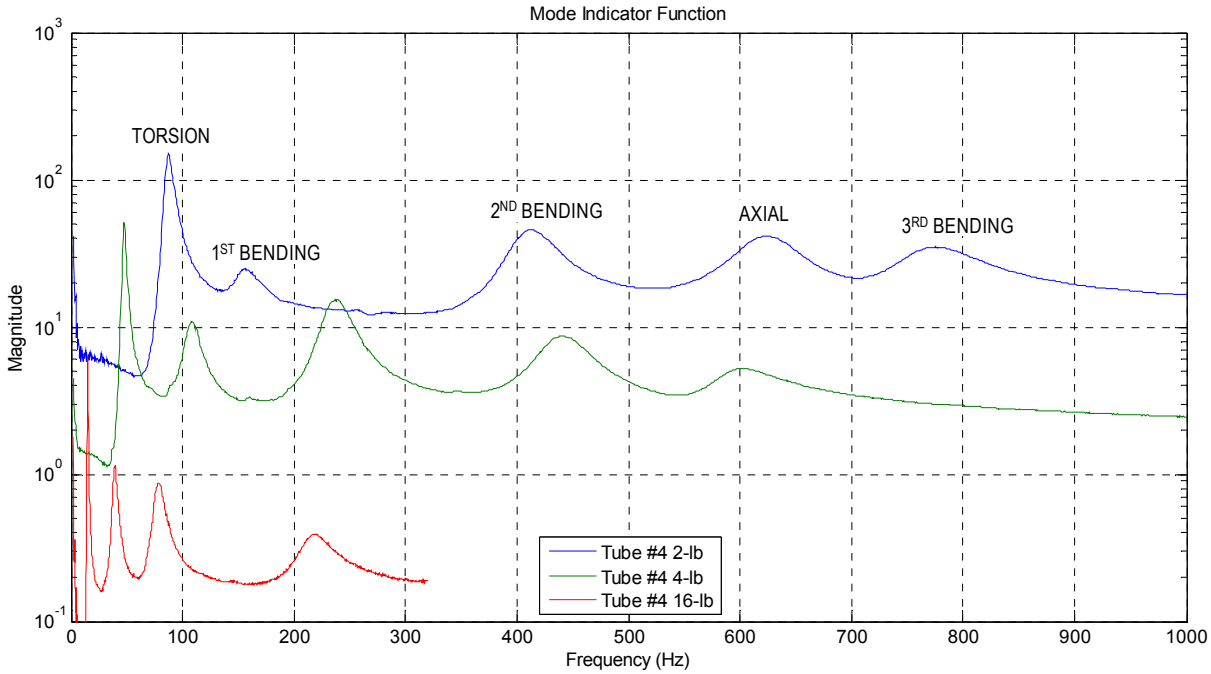

Figure 12. PSMIF from the three configurations for Tube #4.

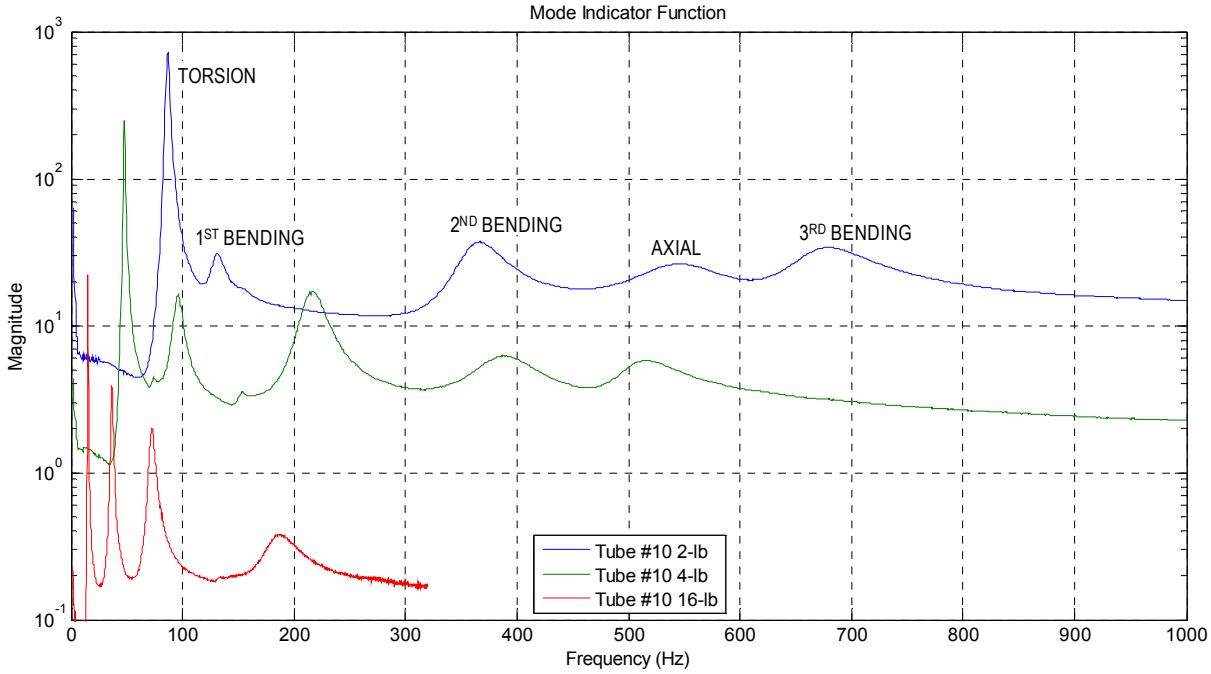

Figure 13. PSMIF from the three configurations for Tube #10.

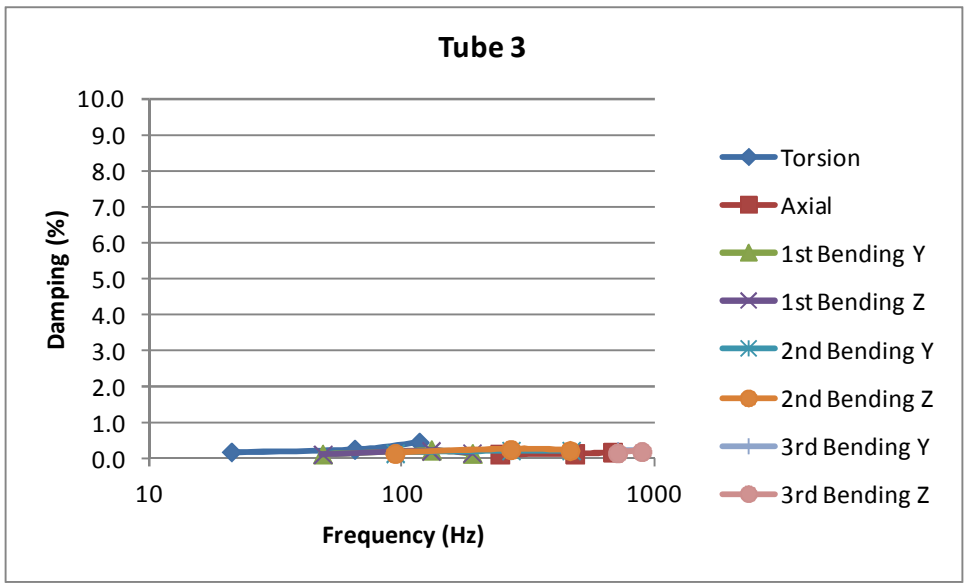

Figure 14. Frequency and damping of all modes from the three configurations for Tube #3.

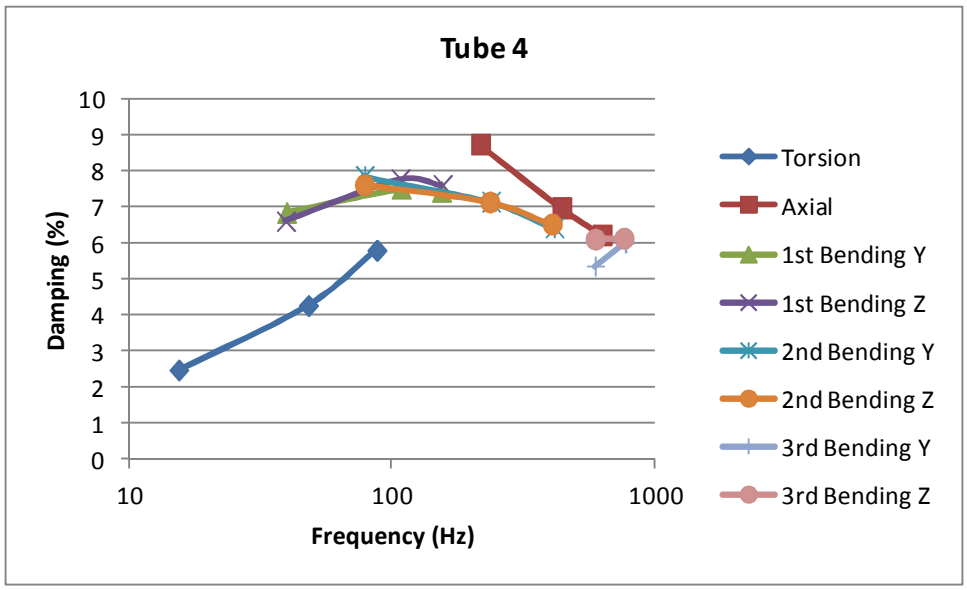

Figure 15. Frequency and damping of all modes from the three configurations for Tube #4.

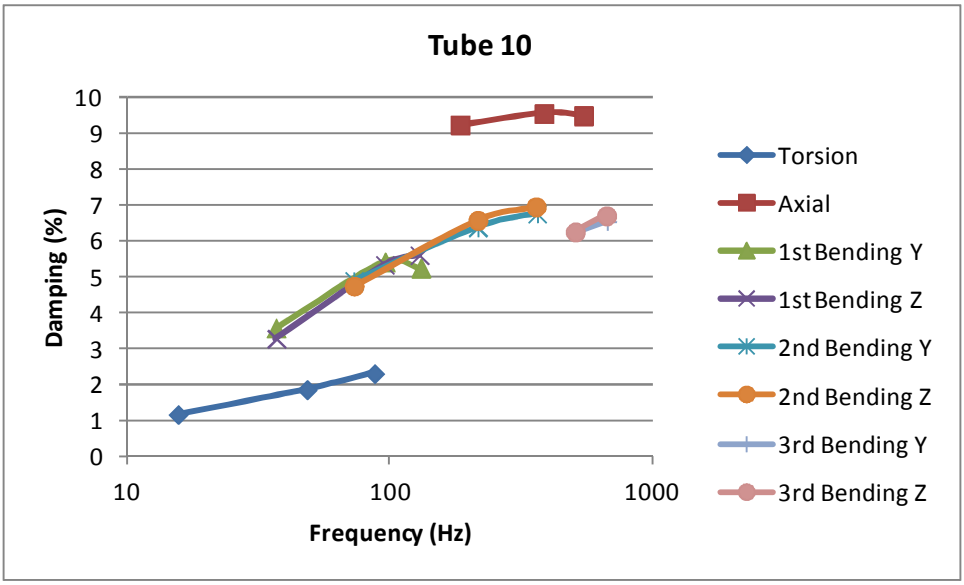

Figure 16. Frequency and damping of all modes from the three configurations for Tube #10.

Table 2: Torsion mode frequency and damping

Tube Number	2-lb Configuration		4-lb Configuration		16-lb Configuration	
	Frequency (Hz)	Damping (%)	Frequency (Hz)	Damping (%)	Frequency (Hz)	Damping (%)
3	115.8	0.47	64.2	0.27	20.9	0.20
4	86.6	5.79	47.5	4.26	15.3	2.47
10	86.6	2.30	48.0	1.86	15.5	1.17

Table 3: 1st bending Y-direction mode frequency and damping

Tube Number	2-lb Configuration		4-lb Configuration		16-lb Configuration	
	Frequency (Hz)	Damping (%)	Frequency (Hz)	Damping (%)	Frequency (Hz)	Damping (%)
3	188.3	0.16	129.5	0.25	48.0	0.14
4	152.6	7.43	107.0	7.52	39.2	6.84
10	130.1	5.24	95.0	5.41	36.5	3.57

Table 4: 1st bending Z-direction mode frequency and damping

Tube Number	2-lb Configuration		4-lb Configuration		16-lb Configuration	
	Frequency (Hz)	Damping (%)	Frequency (Hz)	Damping (%)	Frequency (Hz)	Damping (%)
3	187.4	0.17	129.1	0.23	48.0	0.14
4	154.1	7.61	106.4	7.77	39.0	6.61
10	128.7	5.60	94.9	5.33	36.6	3.27

Table 5: 2nd bending Y-direction mode frequency and damping

Tube Number	2-lb Configuration		4-lb Configuration		16-lb Configuration	
	Frequency (Hz)	Damping (%)	Frequency (Hz)	Damping (%)	Frequency (Hz)	Damping (%)
3	463.7	0.24	268.0	0.24	93.0	0.16
4	409.7	6.43	235.6	7.15	77.9	7.86
10	361.5	6.76	214.6	6.37	72.4	4.88

Table 6: 2nd bending Z-direction mode frequency and damping

Tube Number	2-lb Configuration		4-lb Configuration		16-lb Configuration	
	Frequency (Hz)	Damping (%)	Frequency (Hz)	Damping (%)	Frequency (Hz)	Damping (%)
3	458.3	0.24	267.2	0.26	93.0	0.16
4	401.7	6.53	232.8	7.14	77.6	7.61
10	357.5	6.95	214.3	6.57	72.4	4.74

Table 7: Axial mode frequency and damping

Tube Number	2-lb Configuration		4-lb Configuration		16-lb Configuration	
	Frequency (Hz)	Damping (%)	Frequency (Hz)	Damping (%)	Frequency (Hz)	Damping (%)
3	677.1	0.19	479.4	0.15	241.4	0.13
4	622.1	6.22	436.9	6.97	214.7	8.74
10	541.9	9.48	383.6	9.54	183.8	9.23

Table 8: 3rd bending Y-direction mode frequency and damping

Tube Number	2-lb Configuration		4-lb Configuration		16-lb Configuration	
	Frequency (Hz)	Damping (%)	Frequency (Hz)	Damping (%)	Frequency (Hz)	Damping (%)
3	889.2	0.22	709.0	0.23		
4	764.3	6.01	586.3	5.35		
10	667.6	6.54	504.2	6.24		

Table 9: 3rd bending Z-direction mode frequency and damping

Tube Number	2-lb Configuration		4-lb Configuration		16-lb Configuration	
	Frequency (Hz)	Damping (%)	Frequency (Hz)	Damping (%)	Frequency (Hz)	Damping (%)
3	883.1	0.21	708.2	0.17		
4	753.5	6.13	585.7	6.10		
10	663.5	6.70	504.4	6.25		

MODEL IMPLEMENTATION

It is desired to estimate what kind of an effect can be made in a real world system with increased damping from the wavy composite material. To that end, a composite structure system was chosen as the candidate real-world structure. The system had been previously designed, analyzed, and tested. A well-developed finite element analysis (FEA) model already existed. The peak response values of the system at the components were well understood. It is assumed that the structural modes of the system would not change in frequency with the wavy composite material in place of the original material. The only assumed effect would be an increase in modal damping. The output responses would then be evaluated to determine the effect.

The nominal damping schedule used to analyze the system assumed a default value of 4% modal damping except where experimental modal data existed for the system. In these cases, the modal damping was updated to the test-measured value. Using the experimental modal data of the damped wavy composite material as described in the detailed testing results above, an updated system-level damping table was computed for the system to be used in analysis. From that test data, 8% modal damping was picked to gauge the effect of the wavy composite material on the system responses.

The increase in modal damping from 4% to 8% cannot be an “across-the-board” change where all modes of the system have 8% modal damping. The increase in damping could only be applied to the modes where the wavy composite material would be engaged. The level of engagement was determined by computing the modal strain energy in the candidate composite structure and comparing that to the total strain energy of the system on a mode-by-mode basis. The ratio indicated how active the candidate components were in the system mode, and thus in the

system response. The percent strain energy ratio was used to scale the 8% modal damping value such that the appropriate increase in modal damping could be applied at the system level, to each system mode. The nominal and updated system modal damping schedule can be seen in Figure 17.

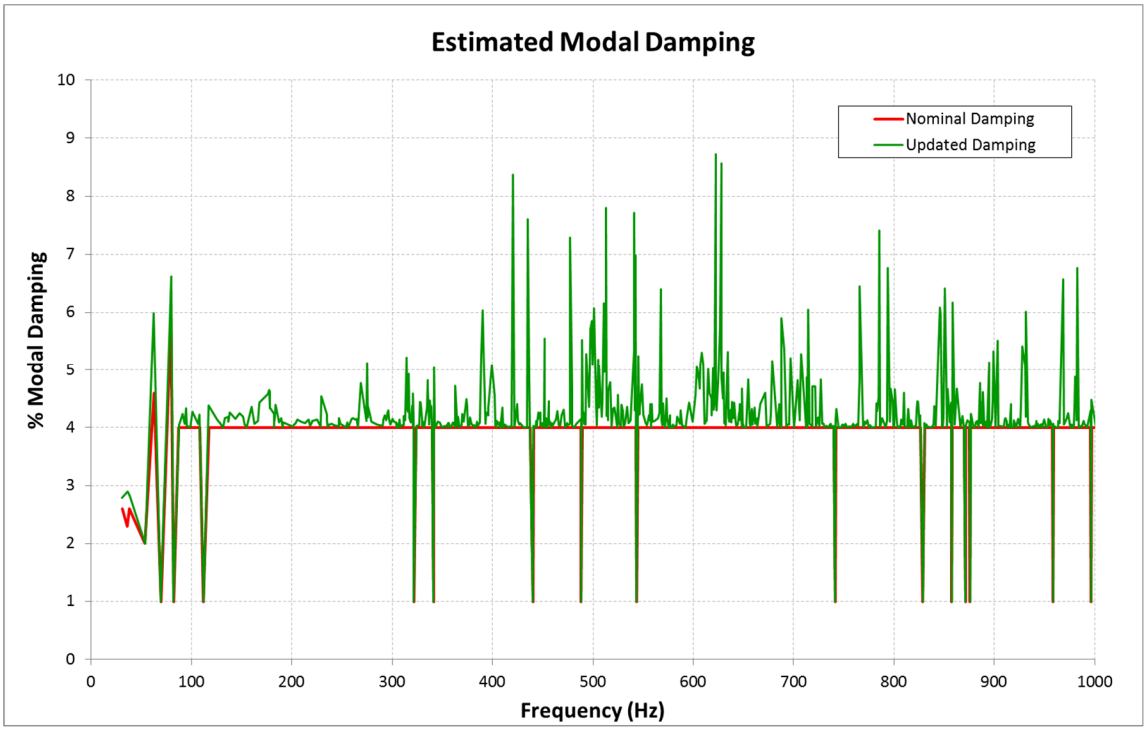

Figure 17. Updated modal damping schedule for analysis

The random vibration and acoustic analyses were performed with the updated damping schedule. The updated damping schedule is an important input for calculating the responses in both of these analyses. The effect of the increase in modal damping for the system level analyses was observed as a decrease in the nodal and elemental output responses. The output results from the analyses were processed in the manner, which had been previously defined for the program. The models showed some reduction in the loads for all components as seen in Table 10. The more significant reductions were seen on cantilevered components with a maximum dynamic loading reduction of 14%.

Table 10: Design Limit Load (DLL) Table

Description	ID	Random Vibe DLL	Direct Acoustic DLL	Max DLL	DLL Source	% Change
Electical Box 1	34100000	14.49	5.11	14.49	Random Vibe	-0.4%
Secondary mirror	24100000	16.90	40.54	40.54	Direct Acoustic	-3.8%
Secondary mirror mount	24100001	10.05	19.39	19.39	Direct Acoustic	-5.2%
Tertiary mirror	23300000	9.05	19.09	19.09	Direct Acoustic	-7.5%
Fold Mirror A	23400000	15.70	51.85	51.85	Direct Acoustic	-14.1%
Electical Box 2	29100000	11.48	18.81	18.81	Direct Acoustic	-5.3%
Lens Housing	10599901	12.54	5.09	12.54	Random Vibe	-1.2%
Control Board 3	41110000	19.61	4.61	19.61	Random Vibe	-1.3%
Control Board 4	41210000	19.08	5.06	19.08	Random Vibe	-1.1%
Filter wheel 1 ; front	14100000	16.80	7.20	16.80	Random Vibe	-1.7%
Filter wheel 1, rear	13100000	17.51	7.88	17.51	Random Vibe	-1.9%
Lens group C	15100000	14.58	3.85	14.58	Random Vibe	-1.4%
Filter wheel 2	8100000	13.09	8.39	13.09	Random Vibe	-2.3%
Filter wheel 2 controller	16110000	13.06	5.22	13.06	Random Vibe	-1.4%
Fold Mirror B	21100000	9.74	16.40	16.40	Direct Acoustic	-6.6%
Electrical Box 4	35100000	9.39	14.09	14.09	Direct Acoustic	-6.4%

CONCLUSIONS

The damped wavy composite as proposed by Dolgin and manufactured by Pratt is a material worth considering for lightweight composite structures. As demonstrated by the system model described in this paper it is a viable way to reduce structural loads significantly. It would also have the added benefit of improving dynamic positional accuracy as responses to vibration loads will have lower displacements and responses to transient loads will decay much more quickly than in undamped structures.

There are many potential applications for the damped wavy composite material.

- Damped structure for space deployments
- Improved stability for cantilevered structure
- Indy car front wing vibration control
- Acoustic Isolation
- Golf clubs
- Skin for aircraft wings
- Etc.

FUTURE WORK

Several areas of work are in consideration regarding this material. Work is already under way to determine more complete damping profiles than were found in this study. In addition, viscoelastic material properties are temperature dependent. Sandia National Laboratories needs to investigate this dependency further to characterize it with respect to the damping properties of the damped composite material. There is a need for investigations on the constituent parts of the damped wavy composite to determine if there are fiber materials, resins, or viscoelastic materials that can be used that would be better suited for specific applications. Pratt has done some investigating that shows that stronger fibers result in stiffer structures with increased damping. Are there viscoelastic materials with properties that are less temperature dependent that will also provide good damping characteristics? Pratt also showed that damping profiles can be tuned by altering the period of the sinusoid, but this needs further investigation. At the time this paper was written, the machine that Pratt constructed to produce the wavy composite prepreg is non-operational. The machine will need to be reactivated. Sandia is currently looking for funding sources to continue this research and reactivate the prepreg machine.

SUMMARY

A test series was carried out to investigate the damping characteristics of a wavy composite material. The wavy composite material sandwiches a viscoelastic material with graphite layers with long fibers in sinusoidal patterns. The sinusoids on either side of the viscoelastic are spatially 180° out of phase with each other. Tubes of this material were tested and compared to test results of an undamped tube. The damped tubes showed greater damping in all modes by as much as 70 times the damping ratio of the undamped tube. Model results of an existing lightweight composite system predict that using the damping demonstrated by the damped wavy composite material reduced dynamic loads in all components and for cantilevered structures by as much as 14%.

REFERENCES

[1] Dolgin, Benjamin P., "Composite Passive Damping Struts for Large Precision Structures." US Patent No. 5,203,435, NASA, USA, Filed August 31, 1990, Awarded April 20, 1993

[2] Pratt, William F.; Allen, Matthew S.; Skousen, Troy J., "Highly Damped Lightweight Wavy Composite." AFRL-VS-TR-2001-1083